

Analytical Solution Describing Pesticide Volatilization from Soil Affected by a Change in Surface Condition

S. R. Yates* USDA-ARS

An analytical solution describing the fate and transport of pesticides applied to soils has been developed. Two pesticide application methods can be simulated: point-source applications, such as idealized shank or a hot-gas injection method, and a more realistic shank-source application method that includes a vertical pesticide distribution in the soil domain due to a soil fracture caused by a shank. The solutions allow determination of the volatilization rate and other information that could be important for understanding fumigant movement and in the development of regulatory permitting conditions. The solutions can be used to characterize differences in emissions relative to changes in the soil degradation rate, surface barrier conditions, application depth, and soil packing. In some cases, simple algebraic expressions are provided that can be used to obtain the total emissions and total soil degradation. The solutions provide a consistent methodology for determining the total emissions and can be used with other information, such as field and laboratory experimental data, to support the development of fumigant regulations. The uses of the models are illustrated by several examples.

FOR decades, pesticides have played a role in increasing the production of crops and commodities while also improving food quality. At the same time, pesticide use has led to adverse air pollution, ground water contamination, and human toxicity effects from exposure to pesticide vapors. Recent examples of degraded environmental systems include the production of near surface ozone (i.e., smog) due to pesticide volatile organic compound (VOC) emission and chemical reactions in the atmosphere. Both situations can cause significant adverse health effects in people living in agricultural areas.

The role of gas-phase transport and volatilization has been clearly shown to be an important process affecting the environmental fate of pesticides (Jury et al., 1983; Taylor and Spencer, 1990). For some chemicals, volatilization is the most important processes governing transport from soil. Even for moderately volatile pesticides, such as the herbicides triallate (Yates, 2006), metolachlor (Prueger et al., 2005), terbutryn (Taberner et al., 2000), EPTC (Baker et al., 1996), and trifluralin (Majewski et al., 1993), volatilization can contribute significantly to atmospheric emissions.

In California, five of the top 10 active pesticide agents are soil fumigants. In 2005, 15 300 tonnes of fumigant chemicals were applied to soil (California Department of Pesticide Regulation [CDPR], 2005), and, due to their large application rates, soil fumigants have become heavily regulated in an effort to reduce atmospheric levels of ozone.

There is currently a great deal of interest in increasing knowledge of volatilization of pesticides under field conditions. In California, large regions of the state are heavily influenced by agriculture. Pesticide use has the potential to increase VOC emissions to the atmosphere and has become a serious concern in California's interior valleys due to a new federal 8-hr ozone standard. Reduction of VOC loading to the atmosphere can be achieved by reducing pesticide emissions from treated soil, prompting state agencies to develop regulations to control pesticide atmospheric emissions. In general, the control strategies increase the cost of agricultural operations and reduce pest-control options. Therefore, information is needed to ensure that new control strategies are justified based on an anticipated reduction in emissions.

In California, the current methodology used to obtain emission information involves conducting large-scale field experiments and measuring pesticide emissions. Continuous and extensive air sampling of the near-surface atmosphere is essential for generating representative concentration profiles that can be used to estimate the volatilization rate. Also, simultaneous measurements of many

Copyright © 2009 by the American Society of Agronomy, Crop Science Society of America, and Soil Science Society of America. All rights reserved. No part of this periodical may be reproduced or transmitted in any form or by any means, electronic or mechanical, including photocopying, recording, or any information storage and retrieval system, without permission in writing from the publisher.

Published in *J. Environ. Qual.* 38:259–267 (2009).

doi:10.2134/jeq2008.0059

Received 1 Feb. 2008.

*Corresponding author (scott.yates@ars.usda.gov).

© ASA, CSSA, SSSA

677 S. Segoe Rd., Madison, WI 53711 USA

USDA-ARS, U.S. Salinity Lab., Riverside, CA 92507.

soil and/or ambient atmospheric conditions are required for calculating volatilization flux using methods such as the aerodynamic method, the theoretical profile shape, and integrated horizontal flux method (Denmead et al., 1977; Wilson et al., 1982; Majewski et al., 1990; Yates et al., 1996).

There are significant difficulties using field experimentation as a basis for creating a consistent set of regulatory decisions, experimental error and uncertainty being most prominent. If field-scale experimentation is used as the sole basis for developing rules governing pesticide use, vast experimental data is needed to ensure statistically and theoretically consistent results. Part of the problem stems from the inability, in an outdoor environment, to isolate single aspects of the fate and transport process. Instead, all processes occurring during the experimental period affect the experimental results. So, for example, if a rule is needed to create permitting conditions based on the emission from deep fumigant application, as opposed to shallow application, field experiments will provide outcomes that include this experimental factor but will also be affected by other complicating soil, chemical, and environmental conditions. When the data are compiled, there is no guarantee that deep-application field experiments conducted at different places and times will provide total emission values that are lower than the experiments conducted with a shallow-application treatment at other places and times. Even though one would expect that experiments conducted in exactly the same way and at the same place and time would demonstrate theoretically correct outcomes, this is not practically possible, so alternative methods are necessary to be certain that regulations are statistically and theoretically consistent.

Pesticide fate and transport models have been used successfully to screen and to categorize pesticides into groups based on their physical-chemical properties and transport behaviors. For example, a screening model was developed (Jury et al., 1983) to assess relative volatility, mobility, and persistence of pesticides in the soil. Other researchers (Rao et al., 1985; Loague et al., 1989) have developed approaches based on the retardation and attenuation factors, allowing pesticides to be categorized based on adsorption and degradation. This can be used to develop approaches to minimize adverse effects as well as to identify potential future problems when new compounds are developed that have similar properties to existing pesticides. A similar approach can be used to assist regulators in developing a theoretically valid set of rules to minimize emission of soil fumigants.

The purpose of this paper is to report on the development of two analytical solutions that could be used by regulators to determine volatilization rates, emission fractions, and the relationship between soil-chemical properties and emissions. This research was motivated by a lack of relatively simple methods available to determine the effect of altering application methods on pesticide efficacy and total emissions into the atmosphere.

Methods

Description of Soil Fumigation Practices

Before fumigation, various tillage operations are conducted to remove any compacted layers between the surface and ap-

proximately 0.75 m (e.g., hard pans) and to break up large soil aggregates that might interfere with fumigant diffusion. This operation tends to create a relatively homogenous soil. A week or two before fumigation, the field is usually irrigated and allowed to drain so that the soil water content is relatively uniform with depth. For hot-gas and shank fumigations, the soil is relatively dry with limited water movement during the fumigation event.

The fumigant is applied using a tractor containing shanks mounted on a tool bar. This provides a series of injection paths (line sources) as the tractor travels down the field. Often, the injection paths are spaced laterally approximately 0.25 to 0.30 m apart. For fumigations that include a surface tarpaulin, the plastic material is carried behind the tool bar and is rolled out over the soil in a continuous operation, producing a continuous high-density polyethylene (HDPE), or other material, cover across the surface of the field.

These fumigant application methods produce symmetrical patterns as shown in Fig. 1, where one shank is presented as either a point source or a rectangular source. For these situations, a source zone is located at the center of the simulated domain and impermeable boundaries occur at the center spacing between nozzles. A volatilization boundary condition is used at the surface, and vertical soil diffusion is assumed to be unlimited.

Model Description

The solutions are intended to describe the transport of a volatile organic chemical (i.e., fumigant, pesticide, or VOC) in a 1-dimensional (vertical) or 2-dimensional soil domain. It is assumed that the water content of the soil is sufficiently low so that water movement over the relatively short time period of the emission event (i.e., weeks) can be neglected and that the soil diffusion coefficient and surface mass transfer coefficient at the soil-atmosphere interface are suitable constants representing the conditions during a fumigation event.

To characterize movement in porous media, an equation is necessary to describe vapor diffusion (Bear, 1972), along with appropriate initial and boundary conditions. For volatile organic chemicals, an appropriate transport equation is

$$\begin{aligned} \frac{\partial \theta C}{\partial t} + \frac{\partial \rho_b S}{\partial t} + \frac{\partial \eta G}{\partial t} &= \frac{\partial}{\partial x} \left[D_L \frac{\partial C}{\partial x} + D_G \frac{\partial G}{\partial x} \right] \\ &+ \frac{\partial}{\partial z} \left[D_L \frac{\partial C}{\partial z} + D_G \frac{\partial G}{\partial z} - qC \right] \\ &- \mu_L \theta C - \mu_s \rho_b S - \mu_G \eta G \end{aligned} \quad [1]$$

where x and z are the horizontal and vertical distances (cm), respectively; C , S , and G are the concentrations (g cm^{-3}) for the liquid, solid, and gaseous phases, respectively; D_L and D_G are the liquid and vapor phase dispersion coefficients ($\text{cm}^2 \text{s}^{-1}$), respectively; q is the Darcian flux density; μ is a first-order degradation coefficient (s^{-1}); and θ , ρ_b , and η , respectively, are the water content ($\text{cm}^3 \text{cm}^{-3}$), bulk density (g cm^{-3}), and the air content ($\text{cm}^3 \text{cm}^{-3}$). The subscripts L , s , and G indicate liquid, solid, and gaseous phases, respectively. The model allows both liquid and vapor diffusion, assumes that volatile solutes are partitioned between the liquid and gas phases following Henry's Law, and that partitioning between

liquid and solid phases follow a linear Freundlich isotherm. Soil degradation is simulated using a first-order decay reaction, and the rate constants can differ in each of the three phases (i.e., liquid, solid, or gaseous).

The total concentration, C_T , is defined as

$$\begin{aligned} C_T(x, z, t) &= \theta C(x, z, t) + \rho_b S(x, z, t) + \eta G(x, z, t) \\ &= R_L C(x, z, t) = R_G G(x, z, t) \end{aligned} \quad [2]$$

The soil-atmosphere boundary condition is described using

$$\left(-D_E \frac{\partial C}{\partial z} + qC \right) \Big|_{z=0} = -b \left(G - G_{air} \right) \Big|_{z=0} \quad [3]$$

where b is a mass transfer coefficient (cm s^{-1}), q is the Darcian flux density (cm s^{-1}), $D_E = (D_L/R_L + D_G/R_G)$ is the effective dispersion coefficient with $D_L = (\theta^{(10/3)}/\theta_s^2) D_{water}$, $D_G = (\eta^{(10/3)}/\theta_s^2) D_{air}$, K_H is the Henry's Law constant, $R_L = (\theta + \rho_b K_d + \eta K_H)$ is the liquid-phase retardation coefficient, and $R_G = R_L/K_H$. Since the soil is relatively dry during fumigation, the Darcian flux, q , is assumed to be zero. Lastly, G_{air} is the gas concentration in the atmosphere above a stagnant boundary layer at the soil surface and is also assumed zero.

The mass transfer coefficients (Jury et al., 1983) are defined as

$$H_E = \frac{b}{R_G}; \quad b = \frac{D_g^{air}}{b} \quad [4]$$

where b is the thickness (cm) of a stagnant boundary layer located at the soil surface and D_g^{air} is the binary diffusion coefficient for the chemical in pure air. The thickness of the boundary layer controls vapor transport away from the soil surface. In Eq. [4], the boundary-layer thickness, b , embodies the processes that affect the transport of a chemical across the soil-atmosphere interface.

The Concentration-time Index

A concentration-time index, C_{Time} , is a useful means for determining the potential effectiveness of pesticide application. The concentration-time gives a method to assess the effect of an organism's exposure to toxic material. With knowledge of the relationship between exposure and mortality, C_{Time} can be used to predict the effectiveness of pesticide application. The concentration-time index (Goring, 1962) is defined as

$$C_{Time}(x, z, t) = \int_0^t C_T(x, z, \tau) d\tau \quad [5]$$

and the total (i.e., maximum value) concentration-time index is the limit as $t \rightarrow \infty$.

Solution Method

For an important class of 2-D or 3-D problems, a multi-dimensional solution for chemical transport can be obtained from multiplying the solutions to the associated 1-D problems (Carslaw, 1959, see Section 1.15). That is, the solution for fumigant transport in a 2-D vertical plane can be obtained using

$$C_T(x, z, t) = C_{T,x}(x, t) C_{T,z}(z, t) \quad [6]$$

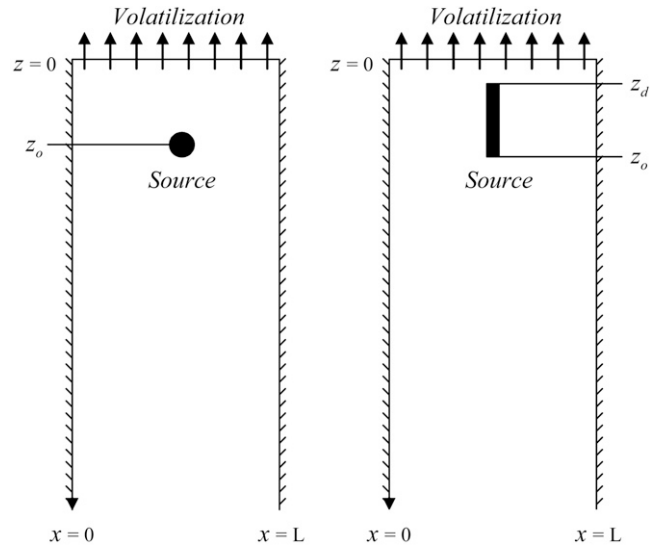


Fig. 1. Schematic of a fumigation system. Hatch marks indicate an impermeable (i.e., reflective) boundary as a result of local symmetry. A fumigant is injected inside the domain $0 \leq x \leq L$ and $0 \leq z \leq \infty$, diffuses in soil, and volatilizes from the surface. A shank moving through the soil causes a rectilinear disturbed zone to a depth z_d . The soil is disked after shank application, which eradicates the disturbance to a depth z_d .

The validity of Eq. [6] can be easily shown by incorporation into Eq. [1] and simplifying. Furthermore, it can be shown that Eq. [6] is a solution when the boundary conditions have the following generalized form

$$\alpha_x \frac{\partial C_{T,x}(x, z, t)}{\partial x} - \beta_x C_{T,x}(x, z, t) = 0 \quad [7]$$

This approach simplifies the development of analytical solutions since it allows a variety of 1-D problems to be combined to provide solutions in two dimensions.

Solution for Transport in the Horizontal Direction

An appropriate 1-D governing equation and boundary conditions for pesticide transport in the horizontal direction (i.e., x) is

$$\begin{aligned} \frac{\partial C_{T,x}}{\partial t} = D_E \frac{\partial^2 C_{T,x}}{\partial x^2}; \quad \frac{\partial C_{T,x}}{\partial x} \Big|_{x \rightarrow 0} = 0; \quad \frac{\partial C_{T,x}}{\partial x} \Big|_{x \rightarrow L} = 0; \\ C_{T,x}(x, 0) = f(x) \end{aligned} \quad [8]$$

Due to the nature of the solution method, the degradation term can be included in both partial differential equations (i.e., x and z directions) as $(\mu/2) C_T$ or can be included in only one of the partial differential equations as the term μC_T . The latter approach has been adopted herein so that the solution for the vertical direction can be directly used for 1-D problems. A general solution to Eq. [8] is

$$\begin{aligned} C_{T,x}(x, t) &= \frac{1}{L} \int_0^L f(\xi) d\xi \\ &+ \frac{2}{L} \sum_{n=1}^{\infty} \left(\int_0^L f(\xi) \cos(k_n \xi) d\xi \right) e^{-D_E k_n^2 t} \cos(k_n x) \end{aligned} \quad [9]$$

where L is the distance between shanks (cm), k_n are the eigenvalues, and $f(x)$ describes the initial concentration in the x direction.

Solution for Transport in the Vertical Direction

An appropriate governing equation and boundary conditions for pesticide transport in the vertical direction (i.e., z) is

$$\frac{\partial C_{T,z}}{\partial t} = D_E \frac{\partial^2 C_{T,z}}{\partial z^2} - \mu C_{T,z}$$

$$D_E \frac{\partial C_{T,z}}{\partial z} \Big|_{z \rightarrow 0} = H_E C_{T,z}(0, t)$$

$$\frac{\partial C_{T,z}}{\partial z} \Big|_{z \rightarrow \infty} = 0$$

$$C_{T,z}(z, 0) = g(z) \quad [10]$$

where $g(z)$ describes the initial fumigant concentration in the vertical direction.

A general solution to Eq. [10] can be obtained using Green's functions (Haberman, 1983):

$$C_{T,z}(z, t) = \int_0^\infty \int_0^\infty G(z, t, \xi, \tau) S(\xi, \tau) d\xi d\tau \quad (\text{Source Term})$$

$$+ D_E \int_0^t \left(G(z, t, \xi, \tau) \frac{\partial C_T(\xi, \tau)}{\partial t} - C_T(\xi, \tau) \frac{\partial G(z, t, \xi, \tau)}{\partial t} \right) \Big|_{z=0}^{z \rightarrow \infty} \times d\tau \quad (\text{Boundary Conditions})$$

$$+ \int_0^\infty G(z, t, \xi, 0) C_T(\xi, 0) d\xi \quad (\text{Initial Condition}) \quad [11]$$

Since no source term is considered, $S(z, t)$ is zero, which simplifies evaluation of Eq. [11].

The free-space Green's function for transport in the vertical direction is

$$G_o(z, t, \xi, \tau) = e^{-\mu(t-\tau)} \left(\frac{e^{-\frac{(z-\xi)^2}{4D_E(t-\tau)}}}{2\sqrt{D_E\pi(t-\tau)}} - \frac{e^{-\frac{(z+\xi)^2}{4D_E(t-\tau)}}}{2\sqrt{D_E\pi(t-\tau)}} \right) \quad [12]$$

and satisfies the partial differential equation for an infinite domain. A Green's function that also satisfies the surface boundary conditions is

$$G(z, t, \xi, \tau) = e^{-\mu(t-\tau)} \left(\frac{e^{-\frac{(z-\xi)^2}{4D_E(t-\tau)}} + e^{-\frac{(z+\xi)^2}{4D_E(t-\tau)}}}{2\sqrt{D_E\pi(t-\tau)}} - \frac{H_E}{D_E} e^{\frac{H_E^2(t-\tau)}{D_E} + \frac{H_E(z+\xi)}{D_E}} \operatorname{Erfc} \left[\frac{H_E\sqrt{t-\tau}}{\sqrt{D_E}} + \frac{(z+\xi)}{2\sqrt{D_E(t-\tau)}} \right] \right) \quad [13]$$

Equation [13] forms the basis of the solutions expressed herein.

Solutions for a Point Source Initial Condition

The concentration, total volatilization, and total concentration-time index, respectively, are

$$C_T(x, z, t) = \frac{C_o}{L} \left(1 + 2 \sum_{n=1}^\infty e^{-D_E k_n^2 t} \operatorname{Cos}(k_n x) \operatorname{Cos}(k_n x_o) \right)$$

$$\left(\frac{e^{-\frac{(z-z_o)^2}{4D_E t}} + e^{-\frac{(z+z_o)^2}{4D_E t}}}{2\sqrt{D_E\pi t}} - \frac{H_E}{D_E} e^{\frac{H_E^2 t}{D_E} + \frac{H_E(z+z_o)}{D_E}} \times \operatorname{Erfc} \left[\frac{H_E\sqrt{t}}{\sqrt{D_E}} + \frac{(z+z_o)}{2\sqrt{D_E t}} \right] \right) \quad [14]$$

$$\text{Total Volatilization} = \frac{C_o H_E e^{-\frac{z_o\sqrt{\mu}}{\sqrt{D_E}}}}{H_E + \sqrt{D_E}\sqrt{\mu}} \quad [15]$$

$$\text{Total } C_{Tinc}(x, z) = \frac{C_o}{L\sqrt{D_E}} \left(\frac{e^{-\frac{(z-z_o)\sqrt{\mu}}{\sqrt{D_E}}} + e^{-\frac{(z+z_o)\sqrt{\mu}}{\sqrt{D_E}}}}{2\sqrt{\mu}} - \frac{H_E e^{-\frac{(z+z_o)\sqrt{\mu}}{\sqrt{D_E}}}}{(H_E + \sqrt{D_E}\sqrt{\mu})\sqrt{\mu}} \right)$$

$$+ \frac{C_o}{L\sqrt{D_E}} \sum_{n=1}^\infty \left(\frac{e^{-\frac{(z-z_o)\zeta_n}{\sqrt{D_E}}} + e^{-\frac{(z+z_o)\zeta_n}{\sqrt{D_E}}}}{\zeta_n} \right) \operatorname{Cos} \left[\frac{\pi x}{L} \right] \operatorname{Cos} \left[\frac{\pi x_o}{L} \right]$$

$$- \frac{2H_E C_o}{L\sqrt{D_E}} \sum_{n=1}^\infty \left(\frac{e^{-\frac{(z+z_o)\sqrt{\mu}}{\sqrt{D_E}}} \operatorname{Cos} \left[\frac{\pi x}{L} \right] \operatorname{Cos} \left[\frac{\pi x_o}{L} \right]}{(H_E + \sqrt{D_E}\zeta_n)\zeta_n} \right) \quad [16]$$

Equations for a Rectangular (i.e., Shank) Source

During soil fumigation, the presence of a shank moving through the soil causes an elongated rectilinear disturbed zone to a depth z_o . After the shank passes, the surface soil is disked, eradicating the disturbance to a depth of z_o' , which is usually about 10 to 20 cm. The geometric description of a shank disturbance would be highly complex; however, here it is simply approximated by a rectangle.

The concentration, total volatilization, and total concentration-time index, respectively, are

$$C_T(x, z, t) = \frac{C_o e^{-\mu t}}{2(z_d - z_o)} \times \left(\frac{1}{L} + \frac{1}{d\pi} \sum_{n=1}^{\infty} e^{-D_E k_n^2 t} \frac{\cos(k_n x)}{n} \frac{\sin[k_n(d - x_o)] + \sin[k_n(d + x_o)]}{n} \right) \times \left(\begin{aligned} & \text{Erfc} \left[\frac{z - z_d}{2\sqrt{D_E t}} \right] + \text{Erfc} \left[\frac{z + z_d}{2\sqrt{D_E t}} \right] - \text{Erfc} \left[\frac{z - z_o}{2\sqrt{D_E t}} \right] \\ & - \text{Erfc} \left[\frac{z + z_o}{2\sqrt{D_E t}} \right] - 2 e^{\frac{H_E^2 t}{D_E} + \frac{H_E(z+z_o)}{D_E}} \text{Erfc} \left[\frac{H_E \sqrt{t}}{\sqrt{D_E}} + \frac{(z+z_d)}{2\sqrt{D_E t}} \right] \\ & + 2 e^{\frac{H_E^2 t}{D_E} + \frac{H_E(z+z_o)}{D_E}} \text{Erfc} \left[\frac{H_E \sqrt{t}}{\sqrt{D_E}} + \frac{(z+z_o)}{2\sqrt{D_E t}} \right] \end{aligned} \right) \quad [17]$$

$$\text{Total Volatilization} = \frac{C_o H_E \sqrt{D_E} \left(e^{\frac{-z_d \sqrt{\mu}}{\sqrt{D_E}}} - e^{\frac{-z_o \sqrt{\mu}}{\sqrt{D_E}}} \right)}{(z_o - z_d) (H_E + \sqrt{D_E} \sqrt{\mu}) \sqrt{\mu}} \quad [18]$$

$$\text{Total } C_{T_{ime}}(x, z) = \frac{C_o}{2L(z_d - z_o)} \times \left(\begin{aligned} & \frac{e^{\frac{-(z-z_d)\sqrt{\mu}}{\sqrt{D_E}}} - e^{\frac{-(z-z_o)\sqrt{\mu}}{\sqrt{D_E}}}}{\mu} \\ & + \frac{(H_E - \sqrt{D_E} \sqrt{\mu}) \left(e^{\frac{-(z+z_d)\sqrt{\mu}}{\sqrt{D_E}}} - e^{\frac{-(z+z_o)\sqrt{\mu}}{\sqrt{D_E}}} \right)}{(H_E + \sqrt{D_E} \sqrt{\mu}) \mu} \end{aligned} \right) + \frac{C_o}{2L(z_d - z_o)} \times \left(\begin{aligned} & \frac{e^{\frac{-(z-z_d)\zeta_n}{\sqrt{D_E}}} - e^{\frac{-(z-z_o)\zeta_n}{\sqrt{D_E}}}}{\zeta_n^2} \\ & + \frac{(H_E - \sqrt{D_E} \zeta_n) \left(e^{\frac{-(z+z_d)\zeta_n}{\sqrt{D_E}}} - e^{\frac{-(z+z_o)\zeta_n}{\sqrt{D_E}}} \right)}{(H_E + \sqrt{D_E} \zeta_n) \zeta_n^2} \end{aligned} \right) \Omega_n$$

with

$$K_n = \frac{n\pi}{L}; \quad \zeta_n^2 = D_E K_n^2 + \mu; \quad \Omega_n = \frac{\cos[K_n x] \{ \sin[K_n(d - x_o)] + \sin[K_n(d + x_o)] \}}{d K_n} \quad [19]$$

Changes in Surface Resistance to Volatilization

The Green's function solution provides an easy method to simulate changes in parameters at some time, t_o , after application. For tarp-shank fumigation, a surface tarpaulin is generally removed a few days after application. This has a significant effect on emissions since the diffusion resistance at the soil

surface abruptly changes. The solutions above can be used to simulate these situations as follows:

$$C_T(x, z, t) = \begin{cases} C_x(x, t) \int_0^{\infty} G(z, t, \xi, 0) g(\xi) d\xi \\ \text{(for } t \leq t_o) \\ C_x(x, t) \int_0^{\infty} G(z, t - t_o, \xi, 0) C_{T,z}(\xi, t_o) d\xi \\ \text{(for } t > t_o) \end{cases} \quad [20]$$

Results and Discussion

To calculate a value for the concentration at a specified place and time, either Eq. [14] or Eq. [17] must be evaluated. As a verification step, the 1-D solutions were compared with a finite-element model, Hydrus 1-D (Simunek et al., 2005). This provides a means to verify the methods used to obtain the solutions and to provide evidence that the programming and implementation were error free. Combining graphs of the numerical and analytical solutions on the same page were visually identical; therefore the data are not shown here. In addition, a more rigorous verification step was to incorporate the solutions above into either Eq. [8] or Eq. [10] and use a symbolic mathematical software system (i.e., Mathematica, Wolfram Research, Inc., Champaign, IL) to show that the equations evaluate correctly.

To illustrate the analytical solutions, several examples were constructed based on recent field experiments to measure methyl bromide emissions from a 3.5-ha field covered by high-density polyethylene (HDPE) tarpaulin (Yates et al., 1996) and numerical simulations conducted by Yates et al. (2002). For this experiment (see Table 1), the water content, θ ; porosity, θ_s ; bulk density, ρ_b ; sorption coefficient, K_d ; and Henry's coefficient, K_H ; were, respectively, 0.1, 0.4, 1.5 g cm⁻³, 0.22 cm³ g⁻¹, and 0.25. The values for the model parameters R_G , D_E , μ , and z_o were calculated to be 2.02, 443 cm² d⁻¹, 0.1 d⁻¹, and 25 cm, respectively. Methyl bromide was injected into the soil at 25-cm depth at 240 kg ha⁻¹. The field was covered by a high-density polyethylene tarpaulin which has a value for H_E of 4.5 cm d⁻¹. For a bare soil surface, H_E was 4257 cm d⁻¹, and for a low permeability tarpaulin (VIF), H_E was 0.023 cm d⁻¹.

Shown in Fig. 2 are the predicted total emissions after methyl bromide application from a point source. The total emissions, as a fraction of the amount applied, were calculated by

$$\text{Total Emissions} = \frac{H_E \int_0^{\infty} C_{T,z}(0, \tau) d\tau}{C_o} \quad [21]$$

Figure 2 demonstrates how the solution can be used to determine the effect of several model parameters on the total fumigant emissions.

Effect of Surface Cover Time

In Fig. 2A, the effect of the time interval during which a surface tarpaulin covers the soil surface is presented for the standard HDPE film. Typical fumigations use HDPE films as

Table 1. List of model parameters and values.

Parameter	Description	Value
θ	soil water content	0.1 cm ³ cm ⁻³
θ_s	soil porosity	0.4 cm ³ cm ⁻³
r_b	soil bulk density	1.5 g cm ⁻³
K_d	soil sorption coefficient	0.22 cm ³ g ⁻¹
K_H	Henry's Law coefficient	0.25
μ	first-order degradation coefficient	0.1 d ⁻¹
C_o	mass applied†	72 mg cm ⁻¹
z_o	shank depth	25 cm
z_d	disk depth	10 cm
L	spacing between shanks	25 cm
R_G	gas phase retardation coefficient	2.02
D_E	effective diffusion coefficient	443 cm ² d ⁻¹
H_E	mass transfer coefficients	
	HDPE‡	4.5 cm d ⁻¹
	bare soil	4257 cm d ⁻¹
	VIF#	0.023 cm d ⁻¹

† Mass per distance in the direction of shank travel.

‡ HDPE, high density polyethylene.

VIF, virtually impermeable film.

the surface barrier covering the field for 5 d. The model predicts that approximately 55% of the applied fumigant will escape to the atmosphere. This compares with field measured values that ranged from 64% ($\pm 10\%$) for micrometeorological methods and 58% for flow-through chamber methods. Also shown are the predicted total emissions when a VIF is used. It is clear that using an expensive impermeable film may not be justified if the tarp is removed after 5 d, since the total emissions are only reduced to 47% (i.e., a 15% reduction). However, increasing the cover period to 15 d reduces emissions to 22%, or a 60% reduction. This compares with field measurements that indicate removing a VIF after 5 d (Wang et al., 1997) reduced emissions from 58% ($\pm 8\%$) under HDPE to 38% ($\pm 2\%$) for VIF. Furthermore, removing the VIF 15 d after application reduced fumigant emissions to less than 5% (i.e., 91% reduction). It appears that the methyl bromide degradation rate for this study was somewhat higher than the value used in the simulation. It is also revealed in Fig. 2A that using HDPE or a VIF provides significant benefit in reducing emission when compared to leaving the soil surface bare, which results in 77% emissions.

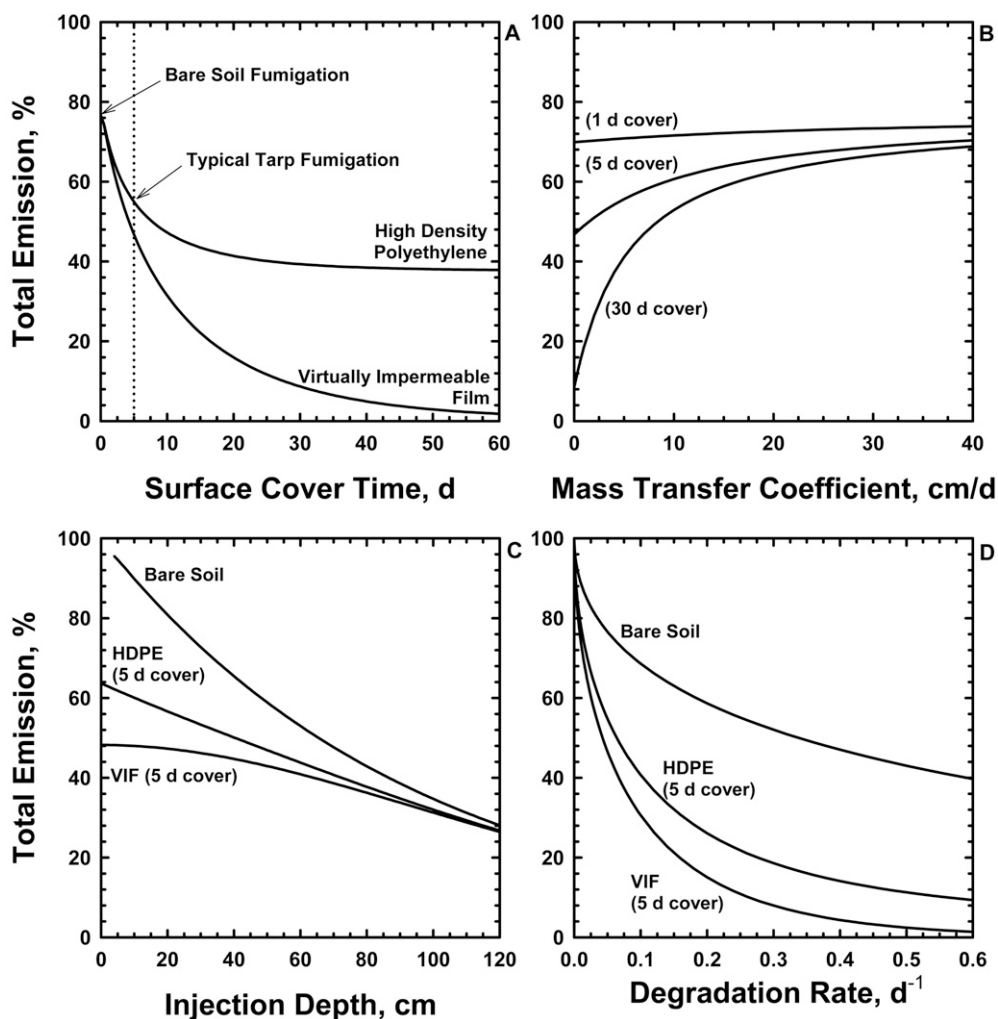


Fig. 2. Example using the model to study the behavior of the emission rate as a function of surface covers time (A), mass transfer coefficient (B), injection depth (C), and degradation rate (D). In (A), the dotted vertical line shows the standard tarp removal time in California. Longer cover periods are needed to achieve substantial emission reduction

This compares with field measurements of 89% (Majewski et al., 1995).

Effect of the Mass Transfer Coefficient

The mass transfer coefficient gives an indication of the resistance to diffusion from the soil into the atmosphere. Various soil and application factors can affect the mass transfer coefficient and include use of films, soil-water seals, and soil compaction, to name a few. Shown in Fig. 2B are predicted total methyl bromide emissions for 1, 5, and 30-d cover periods and a range of H_e . After the cover period, the soil surface is assumed to be bare and has a mass transfer coefficient, H_e , of 4257 cm d⁻¹. For standard HDPE, the mass transfer coefficient, h , has been measured at 9.12 cm d⁻¹ (Papiernik et al., 2001) and the value for a VIF film has been estimated to be more than 200 times less than HDPE (Wang et al., 1999). For very short cover periods, the mass transfer coefficient has little influence on the total emissions. For longer cover periods, significant reductions in emission can be obtained by utilizing management practices that reduce the mass transport coefficient (i.e., surface water seals, impermeable plastic films, and soil compaction).

Effect of the Injection Depth

It has been long known that applying fumigants deeper in soil reduces total emissions to the atmosphere. This is shown clearly in Fig. 2C for bare soil and for 5-d HDPE and VIF surface covers. Typical methyl bromide fumigation under HDPE occurs at approximately 25-cm depth. Increasing the application depth to 68 cm reduces total predicted emissions from 55% to 41%, a 25% reduction. As the injection depth increases, the surface boundary resistance becomes less important. Although not practical in most agronomic settings, nearly identical results occur for injection depths that exceed 1 m.

Effect of the Degradation Rate

The fumigant degradation rate strongly affects the total emissions to the atmosphere. This is clearly presented in Fig. 2D for fumigations conducted with bare soil and HDPE- and VIF-covered surfaces. As expected, without degradation in the soil, total fumigant emissions will always approach 100%. When the soil degradation rate is in the range common to fumigants (i.e., 0.05–0.35 d⁻¹), significant reductions in emissions can occur when using HDPE and VIF covers.

Effect of the Tarpaulin Removal

In most shank fumigation application methods, the surface barrier is removed several days after application. The consequence of removing the surface barrier is seen clearly in Fig. 3, where a HDPE or a VIF tarp is removed after 5 d. Before removal, emissions from soil covered by VIF are nearly zero. At removal, there is a large peak emission that occurs because the concentration distribution near the soil surface builds up under the plastic and is quickly dissipated by volatilization. Since the mass transfer coefficient for bare soil is much higher than for HDPE or VIF surfaces, the predicted emission rate could

exceed the early peak. This type of behavior has been observed in laboratory column experiments (Gan et al., 2000), where a significant increase in emissions was observed immediately following removal of the tarp material. Gan et al. (2000) also observed a much higher peak emission during removal for less permeable plastic material.

Clearly, tarp removal has a significant affect on the emission process. For the relatively permeable HDPE, the cumulative emission for the first 5 d after application was 21% of the applied methyl bromide and for the peak 24-h period ($0.6 \leq t \leq 1.6$ d) was 6.1%. During the first hour after tarp removal, 2.4% was lost; this increased to 12.5% by 24 h (i.e., Day 6). For the VIF, total emissions for the 5 d before removing the tarp were less than 0.04%. Cumulative emissions were 4% the first hour after VIF removal and reached 19.1% after 24 h (i.e., $5 \leq t \leq 6$ d). This information would be very useful to determine worker and public safety during and immediately after removal of the plastic. Field-scale fumigations require a more sophisticated analysis that includes the actual time a section of plastic is removed. This would provide a more accurate measure of the health effects. Further, adjusting the timing of plastic removal would allow dilution in the surrounding atmosphere and may provide a mitigation methodology.

The solution also allows prediction of soil pesticide concentration as shown in Fig. 4, where the methyl bromide concentration in a soil profile 30 min after injection is presented. This figure illustrates the effect of the shank in spreading the chemical in the soil and also explains why measured peak emissions often occur sooner than peak emissions predicted with point-source simulations. Pesticide efficacy may also be improved by providing a more uniform concentration distribution in the soil profile. This may be especially important for less mobile pesticides.

Figure 5 shows a comparison of the point- and shank-source simulation and measured methyl bromide data (Yates et al., 1996). The measured soil-gas concentrations were collected approximately 0.75 d after application. The two solutions provide similar soil-gas phase concentrations with depth; however, the shank solution appears to more closely match the concentrations at 25 and 50 cm compared to the point-source solution. A more detailed data set would be required to more accurately investigate the differences between the solutions.

Conclusions

An analytical solution for the transport of volatile pesticides in porous media has been developed for point and shank sources. A numerical solution to the transport equation has been used to check the accuracy of the analytical solutions. The analytical solution may be useful for verifying the numerical accuracy of more comprehensive numerical solutions to the transport equations as well as for investigating some aspects of the transport process in fumigated soil which may be of use in creating regulations on soil fumigation.

The solutions compare reasonably well to field data reported in the literature when using model parameters collected from a

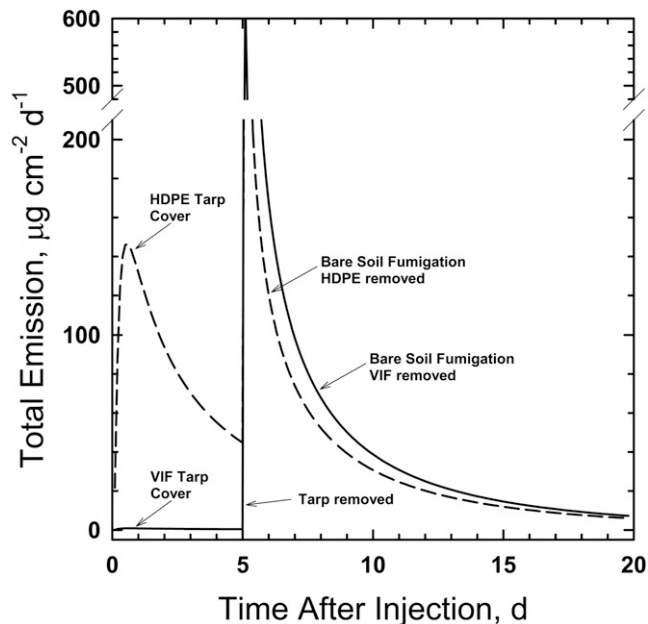


Fig. 3. Example of the emission rate from a field covered with high-density polyethylene (HDPE) and virtually-impermeable film (VIF) for 5 d followed by period of emissions from bare soil.

single field experiment. For some comparisons, improvements could be made if the simulations and comparisons were made

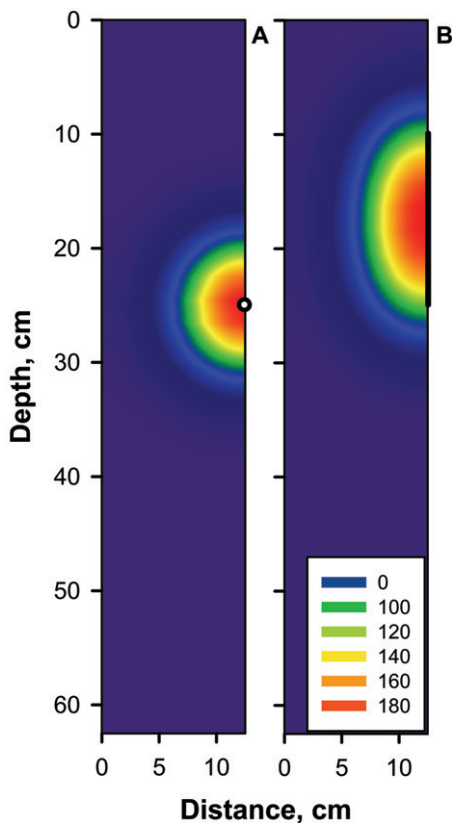


Fig. 4. Simulated methyl bromide concentration ($\mu\text{g cm}^{-3}$) 30 min after injection for a point (A) and shank sources (B). The methyl bromide application rate was 240 kg ha^{-1} and depth of injection 25 cm. The open circle in A and dark line in B indicate, respectively, the position of the injection point and the shank source.

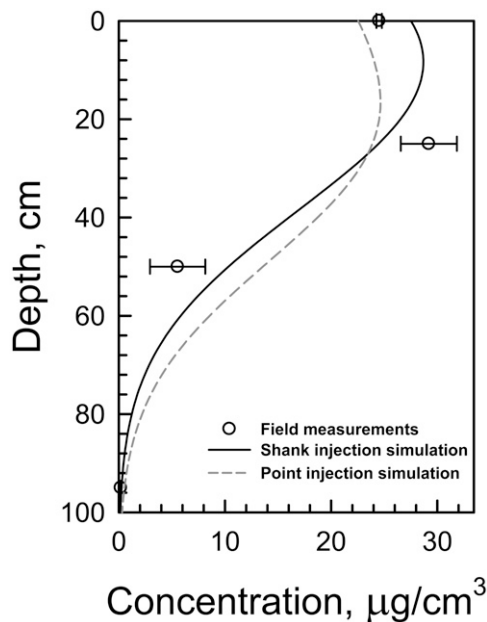


Fig. 5. Predicted and measured methyl bromide gas-phase concentration with depth 0.75 d after application.

using data from their respective experiments. Even without this refinement, the simulations describe the overall behavior observed in the fumigation studies.

Although these solutions should be useful as screening tools, especially when little site-specific data is needed or available, they do not provide a comprehensive description of all the factors that affect fumigant fate and transport. But for regional-scale analyses, which generally lack highly detailed site-specific information, the solutions should provide an appropriate level of detail and useful information for making regulatory decisions.

Acknowledgments

The use of trade, firm, or corporation names in this research article is for the information and convenience of the reader. Such use does not constitute an official endorsement or approval by the United States Department of Agriculture or the Agricultural Research Service of any product or service to the exclusion of others that may be suitable. Funding for this research was from Project No. 06-68390, California Strawberry Commission, Oxnard, CA

References

- Baker, J.M., W.C. Koskinen, and R.H. Dowdy. 1996. Volatilization of EPTC: Simulation and measurement. *J. Environ. Qual.* 25:169-177.
- Bear, J. 1972. *Dynamics of Fluids in Porous Media*. Elsevier, New York.
- Carlsaw, H.S., and J.C. Jaeger, J.C. 1959. *Conduction of heat in solids*, 2nd ed. Oxford Univ. Press, New York.
- California Department of Pesticide Regulation (CDPR). 2005. Top 100 pesticides used statewide (all sites combined) in 2005. CDPR, Sacramento, CA. [Online]. Available at http://www.cdpr.ca.gov/docs/pur/pur05rep/top100_ais.pdf (verified 6 Aug. 2008).
- Denmead, O.T., J.R. Simpson, and J.R. Freney. 1977. A direct field measurement of ammonia emission after injection of anhydrous ammonia. *Soil Sci. Soc. Am. J.* 41:1001-1004.
- Gan, J., S.R. Yates, F.F. Ernst, and W.A. Jury. 2000. Degradation and volatilization of the fumigant chloropicrin after soil treatment. *J.*

- Environ. Qual. 29:1391–1397.
- Goring, C.A. 1962. Theory and principles of soil fumigation. *Adv. Pest Res.* 5:47–84.
- Haberman, R. 1983. Elementary applied partial differential equations with Fourier series and boundary value problems. Prentice Hall, Englewood Cliffs, NJ.
- Jury, W.A., W.F. Spencer, and W.J. Farmer. 1983. Behavior assessment model for trace organics in soil: I. Model description. *J. Environ. Qual.* 12:558–564.
- Loague, K., R.S. Yost, R.E. Green, and T.C. Liang. 1989. Uncertainty in a pesticide leaching assessment for Hawaii. *J. Contam. Hydrol.* 4:139–161.
- Majewski, M.S., R. Desjardins, P. Rochette, E. Pattey, J.N. Seiber, and D.E. Glotfelty. 1993. Field comparison of an eddy accumulation and an aerodynamic-gradient system for measuring pesticide volatilization fluxes. *Environ. Sci. Technol.* 27:121–128.
- Majewski, M.S., D.E. Glotfelty, K.T. Paw, and J.N. Seiber. 1990. A field comparison of several methods for measuring pesticide evaporation rates from soil. *Environ. Sci. Technol.* 24:1490–1497.
- Majewski, M.S., M.M. McChesney, J.E. Woodrow, J.H. Prueger, and J.N. Seiber. 1995. Aerodynamic measurements of methyl bromide volatilization from tarped and nontarped fields. *J. Environ. Qual.* 24:742–751.
- Papiernik, S.K., S.R. Yates, and J. Gan. 2001. An approach for estimating the permeability of agricultural films. *Environ. Sci. Technol.* 35:1240–1246.
- Prueger, J.H., T.J. Gish, L.L. McConnell, L.G. Mckee, J.L. Hatfield, and W.P. Kustas. 2005. Solar radiation, relative humidity, and soil water effects on metolachlor volatilization. *Environ. Sci. Technol.* 39:5219–5226.
- Rao, P.S.C., A.G. Hornsby, and R.E. Jessup. 1985. Indexes for ranking the potential for pesticide contamination of ground water. *Proc. Soil Crop Sci. Soc. Fla.* 44:1–8.
- Simunek, J., M.Th. van Genuchten, and M. Sejna. 2005. The HYDRUS-1D software package for simulating the one-dimensional movement of water, heat and multiple solutes in variably-saturated media. University of California- Riverside Research Reports V3:1–240.
- Tabernerero, M.T., J. Alvarez-Benedi, J. Atienza, and A. Herguedas. 2000. Influence of temperature on the volatilization of triallate and terbutryn from two soils. *Pest Manage. Sci.* 56:175–180.
- Taylor, A.W., and W.F. Spencer. 1990. Volatilization and vapor transport processes. p. 213–269. *In* Pesticides in the soil environment: Processes, impacts, and modeling. Book Series 2. SSSA, Madison, WI.
- Wang, D., S.R. Yates, F.F. Ernst, J. Gan, and W.A. Jury. 1997. Reducing methyl bromide emission with a high barrier plastic film and reduced dosage. *Environ. Sci. Technol.* 31:3686–3691.
- Wang, D., S.R. Yates, J. Gan, and J.A. Knuteson. 1999. Atmospheric volatilization of methyl bromide, 1,3-dichloropropene, and propargyl bromide through two plastic films: Transfer coefficient and temperature effect. *Atmos. Environ.* 33:401–407.
- Wilson, J.D., G.W. Thurtell, G. Kidd, and E. Beauchamp. 1982. Estimation of the rate of gaseous mass transfer from a surface source plot to the atmosphere. *Atmos. Environ.* 16:1861–1867.
- Yates, S.R. 2006. Measuring herbicide volatilizations from bare soil. *Environ. Sci. Technol.* 40:3223–3228.
- Yates, S.R., F.F. Ernst, J. Gan, F. Gao, and M.V. Yates. 1996. Methyl bromide emissions from a covered field: II. Volatilization. *J. Environ. Qual.* 25:192–202.
- Yates, S.R., D. Wang, S.K. Papiernik, and J. Gan. 2002. Predicting pesticide volatilization from soils. *Environmentrics* 13:569–578.